Integration of Artificial Neural Networks in Bridge Load Rating and Case Study Application

Francisco Garcia, B.S.C.E., E.I.
Civil Engineering Department
University of Nebraska-Lincoln
francisco.garcia@huskers.unl.edu

Juan P. Perez Garfías
Civil Engineering Department
Portland State University
jperezg2@pdx.edu

Fayaz Sofi, Ph.D.
Department of Civil Engineering
National Institute of Technology Srinagar, India
sofifayaz@nitsri.ac.in

Joshua S Steelman, Ph.D., P.E.
Civil Engineering Department
University of Nebraska-Lincoln
joshua.steelman@unl.edu

Word Count: 5,780 + 5 tables (250 words per table) = 7,030 words (max 7500)

Submitted August 1st, 2019

ABSTRACT

A large population of aging rural bridges across the United States is reaching and exceeding design service lives. Rural areas, in particular, are populated by older bridges under-designed for modern vehicle demands such as increasingly heavy legal loads, seasonal harvests, and husbandry implements. This situation presents a challenge for bridge managers that must reliably and cost-effectively assess the load carrying capacity of these transportation network assets. Reserve capacity is often available for bridges designed and load rated based on conventional line girder methods. However, it is impossible to assess the benefit from refined analyses or load testing until the investment has been made. This paper presents a methodology for estimating the potential benefit from rigorous methods by using Artificial Neural Networks (ANNs) as a supplementary decision support tool. This paper presents an accompanying case study, illustrating the proposed methodology and the outcome realized through alternate methods of load rating, including ANNs, refined analyses, and diagnostic load testing.

Keywords: Bridge Management, Artificial Neural Networks, Finite Element Modeling, Field Testing.

INTRODUCTION

Although bridges in rural areas of America are out of sight and out of mind for Americans living in large urban centers, these assets form critical links in the transportation network to connect agricultural goods with consumers. Bridge owners must balance economic productivity with operational safety for rural assets that are often old and under-designed for modern loads, such as HL-93, AASHTO and state legal load vehicles, and agricultural husbandry implements. According to the National Bridge Inventory (NBI), 10% of bridges nationally (and 21% of bridges in Nebraska) are load posted to restrict the weight of vehicles crossing the bridge (FHWA, 2015). Many posted bridges were designed and constructed 50 to 100 years ago. The NBI indicates that large proportions (54% nationally, 96% in Nebraska) of posted bridges were designed to "unknown" design loads, typically reflecting that bridge documentation was either not generated or not maintained over time. Additionally, fiscal constraints and economic pressures may prompt bridge owners to adopt policies that push the limits of rural structures. For example, Nebraska state law permits a 15% increase in vehicle loads from standard legal limits during seasonal harvest times.

Therefore, careful assessment of load carrying capacity is essential for older rural bridges. One potential method to reveal inherent capacity and justify higher load ratings is to perform load testing (AASHTO, 2010). However, the potential benefit from load testing is unknown until the cost to perform the load testing has already been incurred. The Bridge Engineering Center at Iowa State University published findings from a series of diagnostic load tests (BEC, 2010). Although the load tests were successful in removing posting from some bridges, the tests were also unable to remove posting for 50% of the tested bridges. Detailed analysis can also justify raising or removal of load restrictions, as an alternative to load testing. AASHTO (2017) designs have traditionally relied on line-girder analysis, but various references (e.g., NSBA G13.1) are available to guide load rating agencies and engineers desiring to identify unacknowledged capacity from refined 3D structural system analysis. Although this guidance exists, a detailed analysis is not guaranteed to provide an accurate answer, and depends strongly on the proficiency of the load rating engineer performing the analysis.

Bridge testing and refined analysis provide valuable tools for bridge management policies, but these capabilities are only sporadically adopted across the United States. According to NCHRP Synthesis 453 (2014), only 24 out of 43 respondents in a state survey indicated that refined analysis was used as part of their load rating policy. Similarly, only 19 of the 43 respondents indicated that load testing was used for load rating. Machine learning and artificial neural networks (ANNs) can provide a supplementary tool to motivate and complement the use of these rigorous load rating methods, and guide bridge management decisions when evaluating aging bridges with low load ratings. Neural network training has become increasingly accessible in recent years. After investing in initial neural network training, a well-trained network can provide a reasonable prediction of the potential benefit available from a bridge test or refined analysis. A neural network can also provide an objective tool for approximately validating refined analysis results. Although machine learning is becoming more commonplace, it is not presently clear how these tools can or should be integrated into bridge management policies.

RESEARCH OBJECTIVE

The objective of this research project is to examine the efficacy of artificial neural networks as part of a comprehensive methodology to assess load capacity for aging bridges and extend service lives for existing inventories. The scope of the project focuses on simple span steel girder bridges, which constitute a large portion of the aging inventory that must be posted to restrict loads. Prior work included performing refined analyses in ANSYS and using the ANSYS data to train committees of neural networks to predict load ratings. The current project examines methods and implications for uncertainty characterization with respect to ANN predictions and field testing validation with case studies.

PROPOSED METHODOLOGY

The proposed methodology builds on a recent guidance document titled Protocol to Evaluate and Load Rate Existing Bridges using Field Testing (Szerszen et al. 2018). This document was produced to assist engineers and owners in the determination of whether to invest in load testing. The proposed methodology is outlined in the flowchart shown in Figure 1, which was modified from the report by Szerszen et al. The proposed methodology was developed with the goal of removing unnecessarily conservative load postings from bridges, and combines the steps for removing a load posting described in the Manual for Bridge Evaluation (MBE) with the intermediate step of reviewing ANN load ratings.

As noted in NCHRP Synthesis 453, the vast majority of posted bridges were evaluated using analytical load rating methods. This typically refers to AASHTO load rating using line girder methods. In the proposed methodology, a bridge that has been determined to require posting based on line girder methods, would then be evaluated using ANNs. If the ANN indicates that the bridge would likely have posting removed by performing refined analysis or load testing, then the bridge owner can prioritize assets for more rigorous investigation according to the expected benefits (e.g., improved transportation network efficiency, deferred rehabilitation costs). The ANNs' load rating prediction alone is not intended to determine whether a load posting should be removed or not. The ANNs' role in bridge management within the proposed methodology is to assist load rating engineers as a decision support tool.

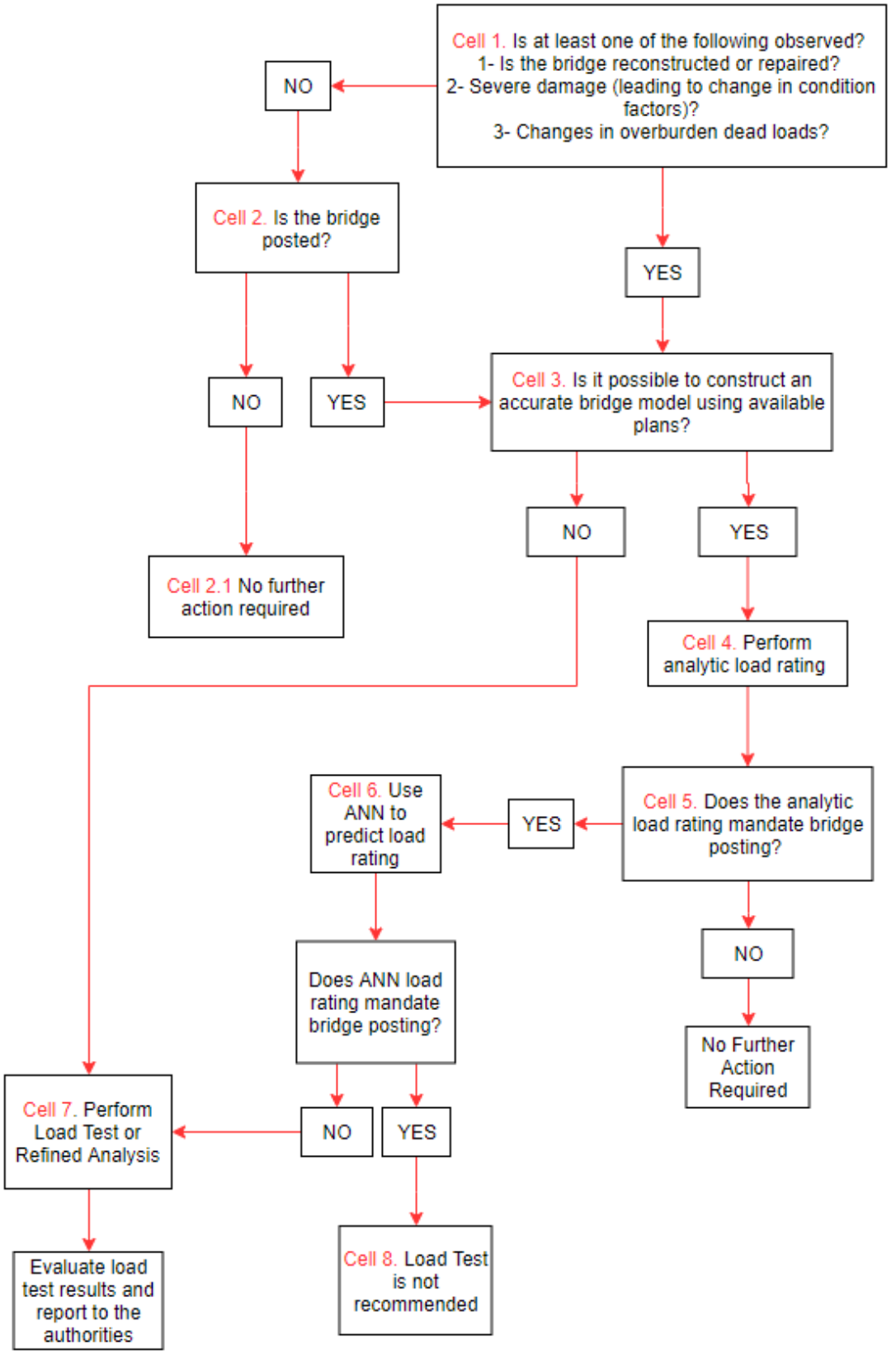

Figure 1. Global Decision Tree

CASE STUDY: YUTAN BRIDGE

Bridge C007805310P was identified as a candidate for a diagnostic load test and is described here as a case study to illustrate how ANNs can be integrated into a bridge management protocol to enhance load ratings. The bridge was constructed in 1981 in Yutan, Nebraska and will be referred to herein as the Yutan bridge. The Yutan bridge supports a rural county road and is owned by Saunders county. Nebraska Department of Transportation (NDOT) records indicated that this bridge should be posted to accommodate special hauling vehicles, and listed an operating load rating of 0.84 based on LFR. The bridge was not constructed with composite connectors, and therefore the documented load rating assumed girders would be governed by noncomposite capacity in flexure.

AASHTO RATING FACTOR

Following the proposed methodology in Figure 1, none of the conditions in Cell 1 applied. Proceeding to Cell 2, the bridge was posted according to NDOT records. Continuing on to Cell 3, the bridge had sparse documentation, but it was possible to perform an analytical load rating, as noted in Cell 4. The analytical load rating was obtained from AASHTO line girder analysis using semi-empirical girder distribution factors (GDFs) from AASHTO LRFD (2016) Section 4, which are well documented to be more conservative than is necessary to satisfy structural reliability. The AASHTO LRFR operating capacity for HL-93 load was calculated to be 0.85, governed by exterior girders.

ANN RATING FACTOR

Because the bridge was posted based on analytical methods, the next step in the proposed methodology is to obtain a rating factor prediction from ANNs (Cell 6). ANNs are tools that can predict an outcome based off of training using similar but different input to the particular point of interest. This study used ANNs that were trained to map 10 governing bridge parameters to corresponding load ratings obtained from refined analyses with finite element models (FEMs), as described by Sofi (2017). The ranges for the governing parameters are shown in Table 1 and serve as the effective range of applicability for the developed ANNs. The parameters for the Yutan bridge are also provided, indicating that the case study bridge has a span length, girder spacing, longitudinal stiffness, number of girders, skew, barrier distance, deck thickness, compressive strength of concrete, and yield strength of steel that are within the appropriate ANN applicability ranges.

Table 1. Yutan Bridge Parameters and Range of Applicability

Governing Parameters and their Effective Ranges.

Bridge Parameters	Effective Range	Selected Bridge Parameters
Span Length (L)	20-89 ft	30.5 ft
Girder Spacing (s)	32-99 in	49.5 in
Longitudinal Stiffness (K_g)	6,200-325,800 in^4	30,306.42 in^4
Cross Frames	Present or Absent	Present
Number of Girders (n_b)	4-11	8
Skew Angle (α)	0-45°	0°
Barrier Distance (d_e)	(-) 8-34 in	7 in
Deck Thickness (t_s)	5-9 in	8.625 in
Concrete Compressive Strength (f_c')	2.5-4 ksi	3 ksi
Steel Yield Stress (f_y)	30-50 ksi	33 ksi

The ANN prediction reflects training conducted using data for 61 bridges extracted from NDOT records, and 193 additional bridge models generated based on hypothetical combinations of bridge governing parameters. The ANNs used in this study were developed using training data for 150 bridges as a design set within the total available set of 254 bridges. FEMs were developed in ANSYS for each bridge using shell elements for steel girders and solid elements for concrete deck, and subjected to simulated truck loading with patch loads to represent tires. The resulting live load response was then used to calculate rating factors, and ANNs were trained to map the governing parameters to rating factors.

ANNs can be trained using different training data, different training set sizes, and different backpropagation algorithms. Changing these variables can affect the reliability of the ANN. Furthermore, the prediction of one ANN may be significantly better than another ANN for the same set of inputs. Because of this, Sofi used committee networks to reduce the average error of load rating predictions. According to Sofi, diversifying the function approximations, network sizes and characteristics, and training subsets provided a more robust load rating prediction.

Sofi compiled four subcommittees with varying numbers of ANNS per subcommittee, two different network architectures, and two different training algorithm. He compared the 99% confidence intervals, mean error, and standard deviation between this ANN and the committee network model for the bridges not used in the design set used to train the ANNs, and observed that the committee ANN had a smaller mean error, smaller confidence interval range, and a smaller standard deviation than the single-best-network, although the differences were relatively minor. The coefficients of correlation between the ANNs and the FEM predictions were found to be .967 and 0.955 for the single-best-network and committee network, respectively.

The FEMs were trained based on ANSYS analyses that assumed composite behavior, and an HS-20 load with no lane load. Accordingly, the ANN rating factors (RFs) needed to be adjusted to 1: convert the inferred live load effect from HS-20 to HL-93, and 2: adjust the assumed capacity from fully composite to noncomposite. The ANN RF is adjusted to account for lane load using Equation 1. A second adjustment was applied as shown in Equation 2 to convert composite capacity to noncomposite capacity.

$$RF_{HS-20,Composite} = RF * \frac{M_{HS-20}}{M_{HS-20} + M_{Lane\ Load}} \quad (1)$$

$$RF_{noncomposite} = RF_{composite} \frac{\varphi C_{noncomposite} - \gamma_{DC} * DC - \gamma_{DW} * DW}{\varphi C_{composite} - \gamma_{DC} * DC - \gamma_{DW} * DW} \quad (2)$$

ANN load ratings were calculated for both the single-best-network and committee network. The single-best network had an adjusted operating load rating of 1.02, and the committee network produced an adjusted load rating of 0.99. These predicted load ratings are marginal and subject to error, but it should be noted that, just as with refined analysis, there is no consideration of nuanced influences such as unintended composite action or boundary restraint.

Calibrated ANN Rating Factor

Sofi (2017) included preliminary statistical analysis to develop a prediction adjustment factor to introduce conservativism to offset uncertainty in ANN RF prediction accuracy. When the ANN prediction is multiplied by the factor, the resulting adjusted prediction shifts to reduce the proportion of the population receiving unconservative RF predictions. Factors were selected to limit the unconservatively predicted population to 1%, 5%, and 10% of the ANN training population.

An alternate preliminary study was performed to account for the additional uncertainty introduced by ANN predictions using structural reliability (Sofi et al. 2019). The study used the Rackwitz-Fiessler method for calibrating partial safety factors (Nowak and Collins 2013). The preliminary calibration found that the inventory capacity live load factor calibrated for the ANN errors in Sofi (2017) was approximately 1.82, or 4% higher than the 1.75 used for inventory ratings in Sofi's ANN training. As shown in Table 2, the reliability approach requires a less severe penalty than the prediction adjustment factors, while maintaining philosophical consistency with LRFD/R. In this table, SBN and CN correspond to single-best-network and committee network, respectively.

Table 2. Calibrated ANN Predictions

	Prediction Adjustment Factor			
	10%	5%	1%	Reliability Method
SBN % Live Load Increase	23.92	16.28	12.61	4.00
CN % Live Load Increase	19.19	13.12	10.25	4.00
SBN RF Scale Factor	0.81	0.86	0.89	0.96
CN RF Scale Factor	0.84	0.88	0.91	0.96
SBN Calibrated RF	0.82	0.88	0.91	0.98
CN Calibrated RF	0.83	0.88	0.90	0.95

FINITE ELEMENT MODELING

The ANN RFs are marginal and slightly less than 1 in the previous section (Cell 6 of the proposed methodology). However, the load rating engineer should recall at this point that the RFs are for LRFR Operating load level with HL-93. Legal loads may rate slightly higher, and result in RFs greater than 1. Additionally, effects such as unintended composite action may contribute significant benefits that are currently unknown. If a load test will be performed, it is also strongly advisable to construct at least a moderately refined model, because the Manual for Bridge Evaluation penalizes, and potentially even negates, the field-measured benefits of load testing if the engineer performing the test cannot explain the source of discrepancies from theory. It was also desirable to perform a validation of the ANN results using detailed analysis to directly investigate prediction error for the case study.

Therefore, the research team constructed refined analysis models in two software packages: ANSYS (Figure 2a) and CSiBridge (Figure 2b). The ANSYS model was constructed similarly to models used for ANN training. Detailed information for the finite element analysis (FEA) modeling methodology is available in Sofi and Steelman (2017). HS-20 loads were modeled for single-lane and two-lane loading cases for interior and exterior girders. The maximum bending effect of the four loading scenarios was taken to be the critical flexure case. The live load was multiplied by the LRFR load factor and amplified for impact according to AASHTO MBE. The exterior girder governed the load rating. The calibrated operating load rating that reflects LRFR loading and noncomposite behavior was found to be 1.04, which is 22% higher than the AASHTO LRFR load rating. The Yutan bridge was also modeled in CSiBridge similarly to ANSYS. Both ANSYS and CSiBridge used shell elements for the steel girders, but CSiBridge also used shells for the deck, rather than solid elements used by ANSYS. CsiBridge automatically computes AASHTO LRFD rating factors, which is convenient, yet more difficult to interrogate. The interior and exterior operating rating factors from the CSiBridge analysis were 1.06 and 0.96 assuming noncomposite behavior.

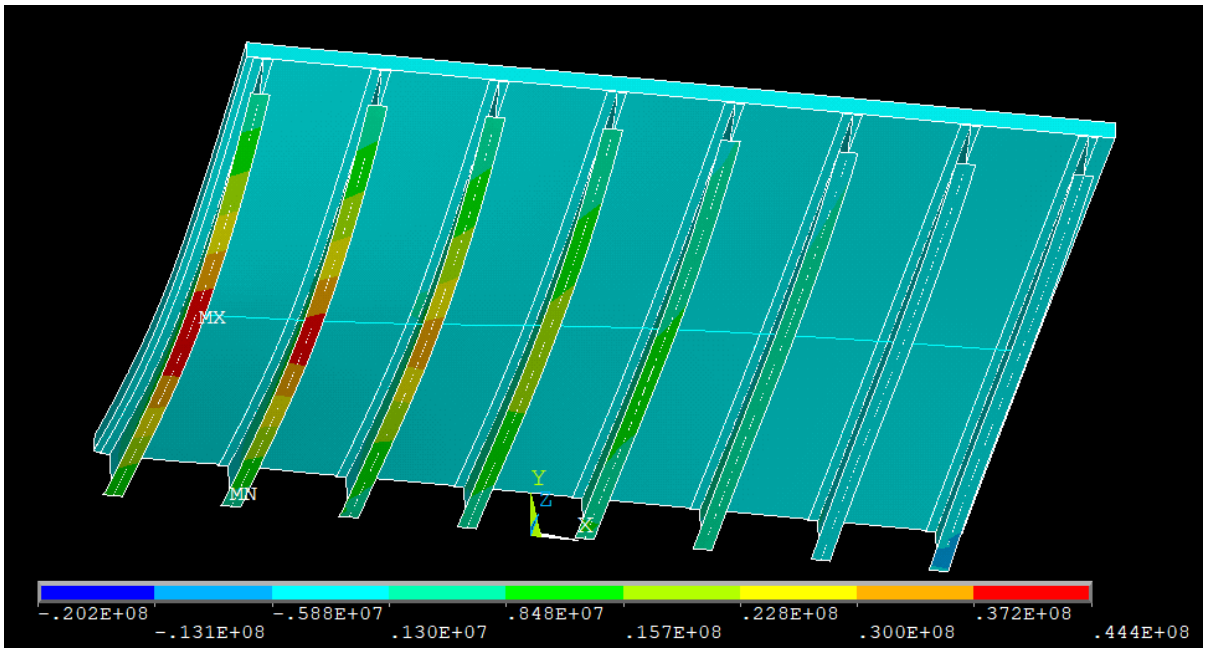

(a)

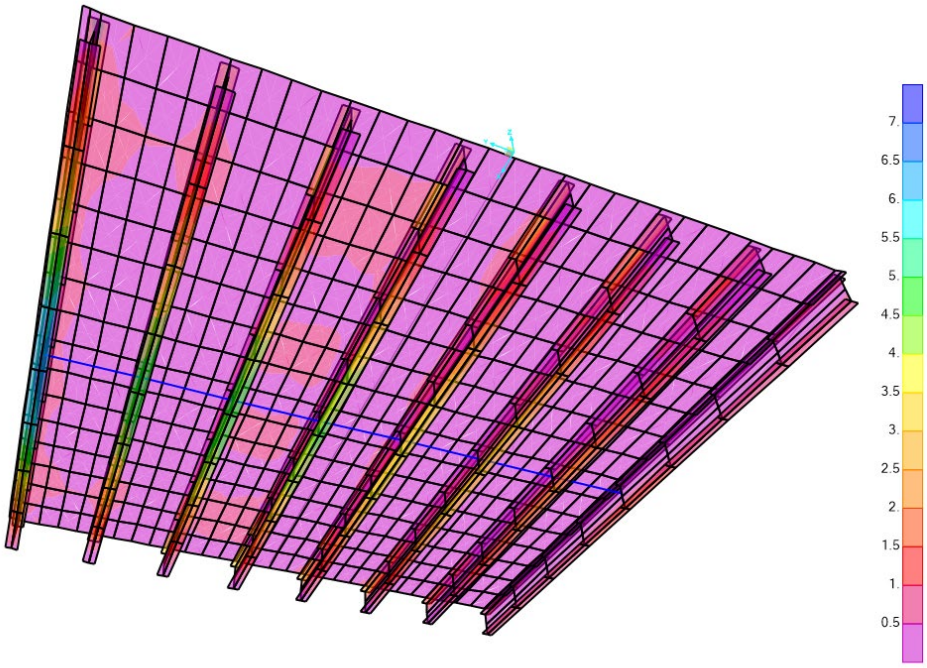

(b)

Figure 2. (a) Stress in ANSYS Model subjected to HS-20 Truck Exterior Single Lane Loading (b) Stress of CSiBridge Model under HL-93 Load

YUTAN BRIDGE LOAD TEST

The CSiBridge and ANSYS RFs disagreed by a noticeable margin, yet both agreed that the load rating at Operating with HL-93 should be either very near or should exceed 1. To obtain the most accurate load rating, and to provide context and a point of reference to the ANN and FEA results, a load test must be performed. A diagnostic bridge test was planned and conducted to investigate the potential benefit from empirically-based effects such as unintended composite behavior and support restraint.

The bridge was instrumented with Bridge Diagnostics Inc. (BDI) strain transducers at girders 1-5 and girder 8 (Figure 3a). Sensors were installed near the abutments as well as at the center of the span (Figure 3b) to investigate both potential restraint and induced negative moments near supports, as well as anticipated critical positive moment. The North abutment was not instrumented at girder 8 due to safety concerns. For the instrumented girders, two strain gauges were installed at the bottom flange and one strain gauge was mounted on the web near the top flange (Figure 3c). Pairs of sensors were installed at bottom flanges to investigate potential lateral bending. To accommodate limitations in the available quantity of sensors, girders 5 and 8 were instrumented to verify symmetric bridge behavior.

Strain gauges were placed about 6 inches to the South of the midspan to avoid a line of diaphragms. Instrumentation near abutments was placed at about 8 inches from supports. The gauge near the North abutment for girder 4 and the gauge near the South abutment for girder 1 were placed about 12 inches from the abutments to avoid small holes cut in the web at the typical instrumentation location. Each strain gauge was installed to capture primary bending effects along the longitudinal direction, in accordance to the BDI user manual.

The BDI software was tared to zero so that only live load strain was recorded. The loading vehicle was driven across the bridge at a crawl speed to mitigate potential dynamic amplification effects. The vehicle was driven along three designated loading paths: critical loading for the exterior girder, critical loading for the interior girder, and along the bridge centerline to verify symmetric structural response to applied load. The vehicle was also driven along the three paths at the posted speed limit for the bridge to investigate dynamic amplification effects. Runs were performed in both directions to ensure two sets of data would be available. The outsides of the tire load paths were painted on the pavement to help guide the truck driver.

(a)

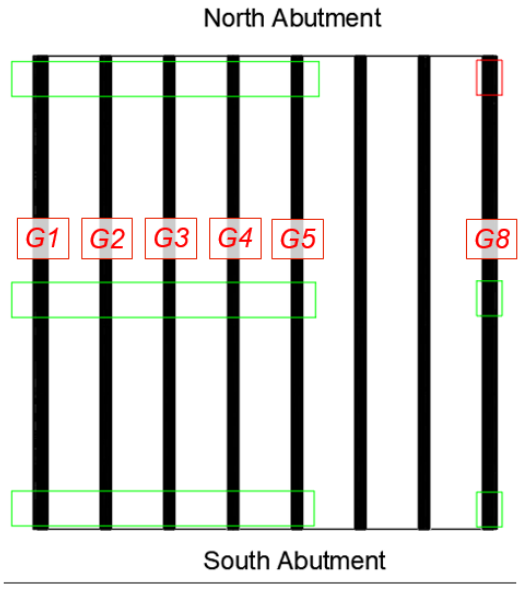

(b)

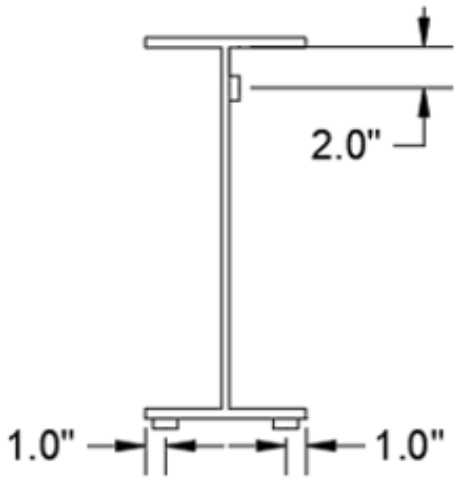

(c)

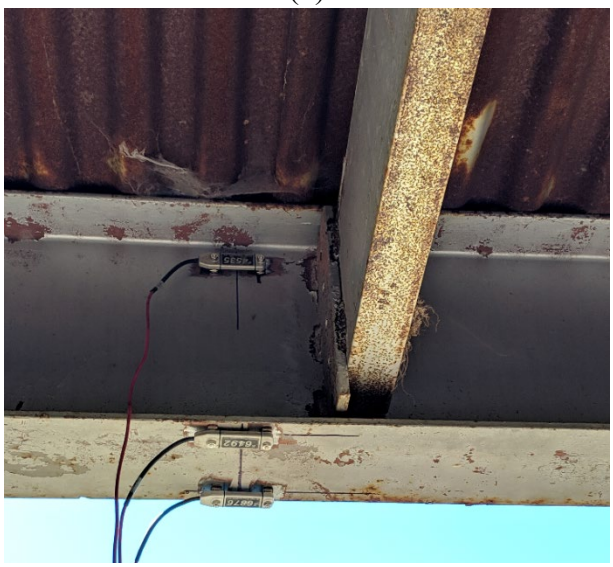

(d)

(e)

Figure 3. Yutan Bridge Instrumentation: (a) Cross Section View (b) Plan View (c) Instrumentation Locations, (d) Site Image of Instrumentation, and (e) Load Vehicle Crossing at Crawl Speed

Although the Yutan Bridge was rated as noncomposite, it was determined that partial composite behavior was present in the bridge based on strain measurements and elastic neutral axis (ENA) location. If the girders were truly noncomposite, then the absolute value of the strain measurements at the top and bottom of the girder would be similar for midspan instrumentation locations. If the bridge was acting perfectly compositely, then the strain gauge near the top flange would be of a smaller magnitude than the bottom flange strains.

The theoretical noncomposite and composite ENA are 9 and 14.86 inches, respectively. Most ENA locations were determined to be between these values, suggesting that there is some degree of composite behavior. It was determined that all of the girders exhibited partial composite behavior, except for girder 2, which had strain distributions that correspond to a noncomposite section. The bridge was built with a corrugated steel deck spanning between the steel girders and separating the girders from the concrete deck. Based on communications with the county engineer regarding local practices at the time of construction of the bridge, it is believed that puddle welds were typically used to hold the steel deck in place while the concrete deck was being placed. Sufficiently detailed construction drawings were not available to confirm the size or spacings of the puddle welds. Since one of the girders was exhibiting noncomposite behavior, it is possible that the bridge has experienced puddle weld deterioration due to overloading. Or, puddle welds may have been omitted at that girder during construction.

Abutment instrumentation locations revealed that there were near zero moments at all of the girders, except for girders 3 and 5. Girders 3 and 5 showed negative bending, which is attributed to higher stiffnesses introduced by nearby H-piles. Other girder ends rested on a pair of channels running past the H-pile flanges. Girders 3 and 5 also exhibited net axial tension in the steel sections. The critical loading scenario is shown in Figure 4. The midspan moment was calculated by solving for the amount of compression in the concrete based on the strains in the steel as well as the net tension effect. The net tension was taken as the average of the axial force at the north and south abutments. Multiple concrete strain distributions were used which created moment ranges for all of the girders in the interior girder loading case. The maximum and minimum moments only differed by 1 to 2 kip-ft for the interior girder load case.

Midspan moment distributions were plotted for pin-roller and pin-pin end restraints for ANSYS and CSiBridge models, as well as moments calculated from the load test. The moment distributions are shown in Figure 5. Although the measured end moments were relatively small, the girder moments appear to be consistent with partial support restraint. Considering the low support moments, and the net axial tension forces, it is believed that transverse stiffening effects along the lengths of the abutments introduced unanticipated stress distributions and load paths.

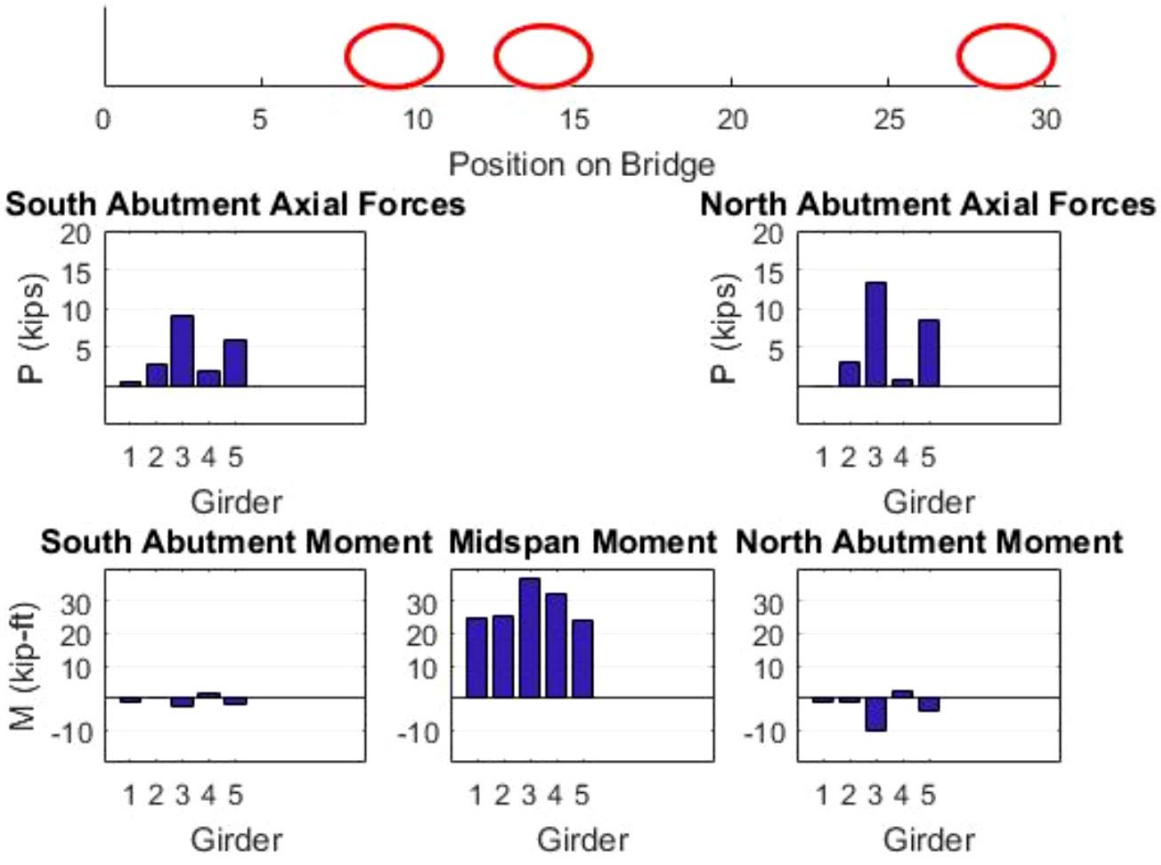

Figure 4. Bridge Respond for Interior Girder Load Case

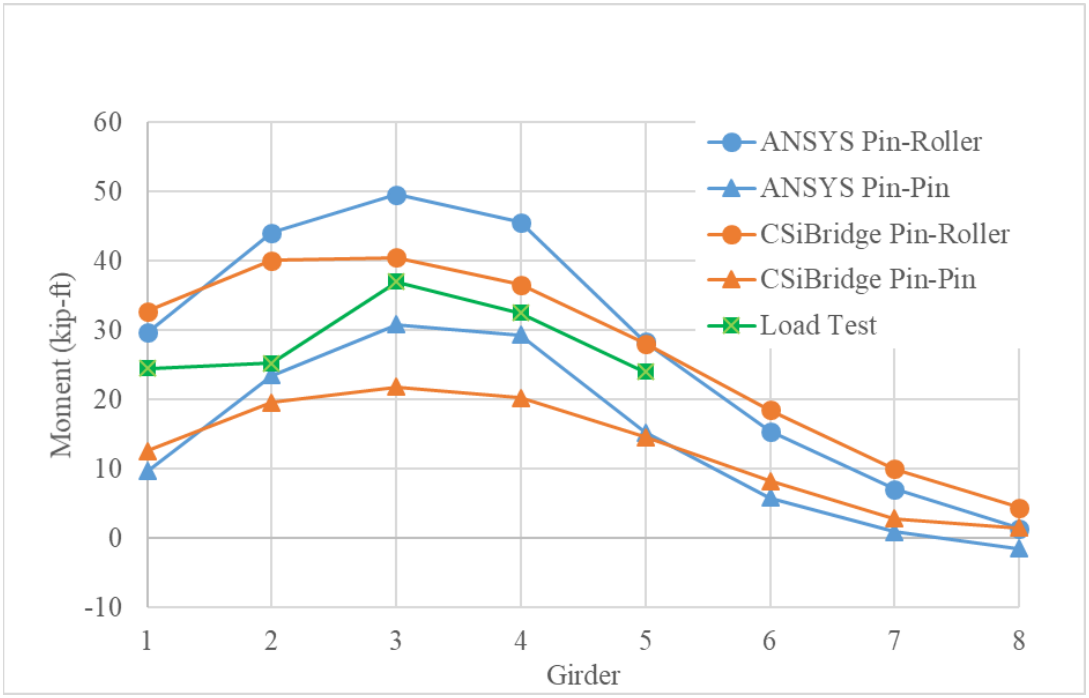

Figure 5. Analytical and Experimental Moment Distributions

Experimental Load Rating

The AASHTO Manual for Bridge Evaluation (MBE 2013) outlines a method for updating load ratings based on experimental load ratings. The general experimental load rating equation is shown below. The subscript "T" denotes data based on testing and the subscript "C" corresponds to values based on calculations. K, in Equation (3) is the adjustment factor for the load rating based on behavior observed from the load test. The overall benefit, K, is impacted by K_a and K_b, as shown in Equation 4. K_a is the direct comparison between theoretical and the load test results, as shown in Equation 5. K_b is a factor that accounts for the understanding of the load test when compared to the theoretical computations. Table 3 shows the appropriate value for K_b, as shown in AASHTO MBE.

$$RF_T = RF_C * K \quad (3)$$

$$K = 1 + K_a K_b \quad (4)$$

$$K_a = \frac{\varepsilon_C}{\varepsilon_T} - 1 \quad (5)$$

Table 3. Recommended Values for K_b

Can member behavior be extrapolated to		Magnitude of test load			K_b
Yes	No	$\frac{T}{W} < 0.4$	$0.4 \leq \frac{T}{W} \leq 0.7$	$\frac{T}{W} > 0.7$	
✓		✓			0
✓			✓		0.8
✓				✓	1
	✓	✓			0
	✓		✓		0
	✓			✓	0.5

The maximum theoretical strain corresponds to the exterior girder being loaded. The maximum experimental strain came from the exterior girder being loaded. The maximum average bottom flange strains for runs 9 and 10 (exterior critical lane path) were 233.9 and 215.9 (με), respectively. Both of those strain measurements corresponded to girder 1 strain measurements. The average of the two bottom flange strain measurements for the two runs were used for ε_T. ε_C, calculated in Equation 6, is based off of theoretical load effect in the member corresponding to ε_T, L_T, the section factor, *SF*, and the modulus of elasticity, *E*. Since the bridge was most likely rated based off of line girder analysis with simply-supported end conditions, L_T was calculated by using the critical moment load placement determined from using influence line analysis and AASHTO exterior girder distribution factors. The section factor is based off of

noncomposite section properties because the bridge was rated as noncomposite. Equation 7 shows the resulting K_a.

$$\varepsilon_C = \frac{L_T}{(SF)E} = \frac{DF * M_{Critical}}{(SF)E} = \frac{0.394 * 233.9\ kipft * \frac{12\ in}{1\ ft}}{87.93\ in^3 * 29{,}000\ ksi} = 434\ \mu\varepsilon \quad (6)$$

$$K_a = \frac{434\ \mu\varepsilon}{208\ \mu\varepsilon} - 1 = 1.08 \quad (7)$$

K_b takes into consideration whether the load test behavior is dependable. The magnitude of the load test was 0.7 of an HS-20 truck. Partial composite behavior may not be dependable, since the load test revealed that some girders were acting noncompositely. According to AASHTO MBE, then, K_b should be taken as either 0.5 or 1.0, depending on whether or not the load rating benefits relative to theoretical calculations can be extrapolated to 133% of the weight of an HS-20 truck. If K_b is taken as 0.5, then K is found to be 1.54. If K_b is taken as 1.0, then K is taken as 2.08. The resulting AASHTO experimental operating rating factors would be 1.32 and 1.77 for $K_b = 0.5$ and $K_b = 1.0$, respectively. In either case, the load test was successful in removing the load posting.

UNCERTAIN COMPOSITE INTERFACE STRENGTH

As noted previously, it is believed that puddle welds were used to connect the steel deck to the girders. Puddle welds are typically neglected as composite connectors for both building and bridge construction. However, AISC does recommend accounting for composite action from deck-to-beam connectors when performing vibration analyses (Murray et al., 1997). Although puddle welds are believed to be the source of composite shear transfer, specific characteristics about the puddle welds at the case study bridge are unknown. These characteristics include the type of electrode used, the effective diameter of the puddle welds, and the spacing between puddle welds along the length of girder. In an effort to explore the implications of the unknown composite shear transfer strength while maintaining philosophical consistency with LRFR, a parametric structural reliability study was conducted to relate rating factors for the critical girder to the mean and uncertainty of the composite interface strength.

The equations utilized to calculate puddle weld strength were obtained from Miller (2017). The equation for effective diameter is

$$d_e = 0.7d - 1.5t$$

and the equation for puddle weld strength is

$$P = \frac{d_e^2 F_{exx}}{4}$$

Where d is the diameter of the puddle weld (in.), t is the thickness of the steel deck (in.), and F_{exx} is the weld metal strength (kips / in^2). Characteristic or ranges of values for each parameter were obtained from literature. Achter (2016) referred to 3/4 in. puddle welds as "ubiquitous". Additionally, the Vulcraft Design Manual (2008) provides diaphragm strength tables based on 5/8 and 3/4 in. diameters. Accordingly, minimum values of 1/2 and 1 in. were arbitrarily selected to bound the typical values. The bridge documentation indicated that the steel deck was approximately 1.5 inches deep, but the deck thickness was not noted. The Vulcraft Manual indicates that 1.5C deck is available in thicknesses from 24 ga (0.0238 in.) to 18 ga (0.0474 in.). The maximum deck thickness listed by Vulcraft for any deck type was 16 ga (0.0598 in.). Electrodes are typically either E60XX or E70XX (Sputo et al., 2010).

Considering these parameter ranges, the minimum nominal shear transfer from the puddle welds would be negligible at only 1 kip for only one 1/2 in. puddle weld in the half span connecting 16 ga steel deck to a steel girder with an E60XX electrode. The maximum nominal shear transfer would be approximately 216 kips for one 1 in. puddle weld in each rib (6.5 in. spacing) along the half span connecting 24 ga steel deck to a steel girder.

The reliability analyses used a dead load nominal moment from a simple beam analysis of the bridge. The live load nominal moment corresponds to an AASHTO GDF analysis for the critical exterior girder under HL-93 load. Nominal resistances were likewise calculated for noncomposite, fully composite, and partially composite capacities for the critical girder. All puddle welds were assumed to have identical strengths at any particular girder. Variation was only considered for the total shear transfer capacity from one random girder to the next. Insufficient experimental documentation has been identified to confidently characterize the composite connection limit state behavior as ductile or brittle. So, alternate scenarios were considered to investigate the implication of this consideration on safe load carrying capacity.

Probability distribution types, bias factors and coefficients of variation (COV) were assumed based on NCHRP Report 454 (1998) and Nowak and Collins (2013), as shown in Table 4.

Table 4. Reliability Analysis Parameters for Uncertain Composite Capacity.

	Nominal (kip-ft)	Bias	COV	Distribution Type
Dead Load	46	1.04	0.08	Normal
Live Load	149	1.00	0.18	Lognormal
Noncomposite Moment Capacity	274	1.07	0.13	Normal
Composite Moment Capacity	595	1.12	0.10	Normal

In the partial composite transition from non- to full composite, bias and COV were assumed to match noncomposite when composite shear strength was less than 50% of the required strength to achieve full composite, and to match fully composite bias and COV otherwise. This partition was selected to be consistent with the Commentary of the American Institute of Steel Construction Specification (2016). Composite shear (puddle weld) strength was assumed to follow a lognormal distribution (Figure 6a) so that combinations of small

strength and large uncertainty would have zero probability of negative composite shear strengths. The puddle weld strength bias factor was assumed to be 1, and the COV was parameterized to range from 0 to 0.5.

When puddle welds were assumed to be brittle, the cumulative density function for composite shear strengths up to the full composite shear strength was assumed to result in puddle weld overload and brittle failure, resulting in noncomposite behavior. Alternatively, the cumulative probability of shear strengths greater than necessary to achieve full composite resulted in full composite strength. Accordingly, the probability distribution for moment capacity with brittle puddle weld limit behavior followed a bimodal distribution (Figure 6b). When ductile limit behavior was assumed at puddle welds (such as yielding in the deck near the puddle weld), the probability distribution for the moment capacity was obtained by combining probability distributions at steps of composite shear strength by the probability of the corresponding shear strength occurring (Figure 6c).

Rating factors were determined by performing a reliability analysis using the Rackwitz-Fiessler method Nowak and Collins (2013) for parametric ranges of mean and COV of composite shear strength, using a limit state function consistent with the AASHTO rating factor equation. The analyses revealed that there was essentially no benefit from composite action if the puddle welds exhibit a brittle limit mechanism (Figure 6d). The potential benefits from a higher mean moment capacity with composite strength were overwhelmed by the excessively large accompanying uncertainty. If the welds exhibit a ductile limit mechanism, the analyses suggest that the Yutan bridge will be able to realize the enhanced strength available from composite action (Figure 6e), and the load rating could potentially increase by 69% to 93% if the mean composite shear strength is 200 kips (near the upper bound estimate mentioned previously), depending on the composite strength uncertainty.

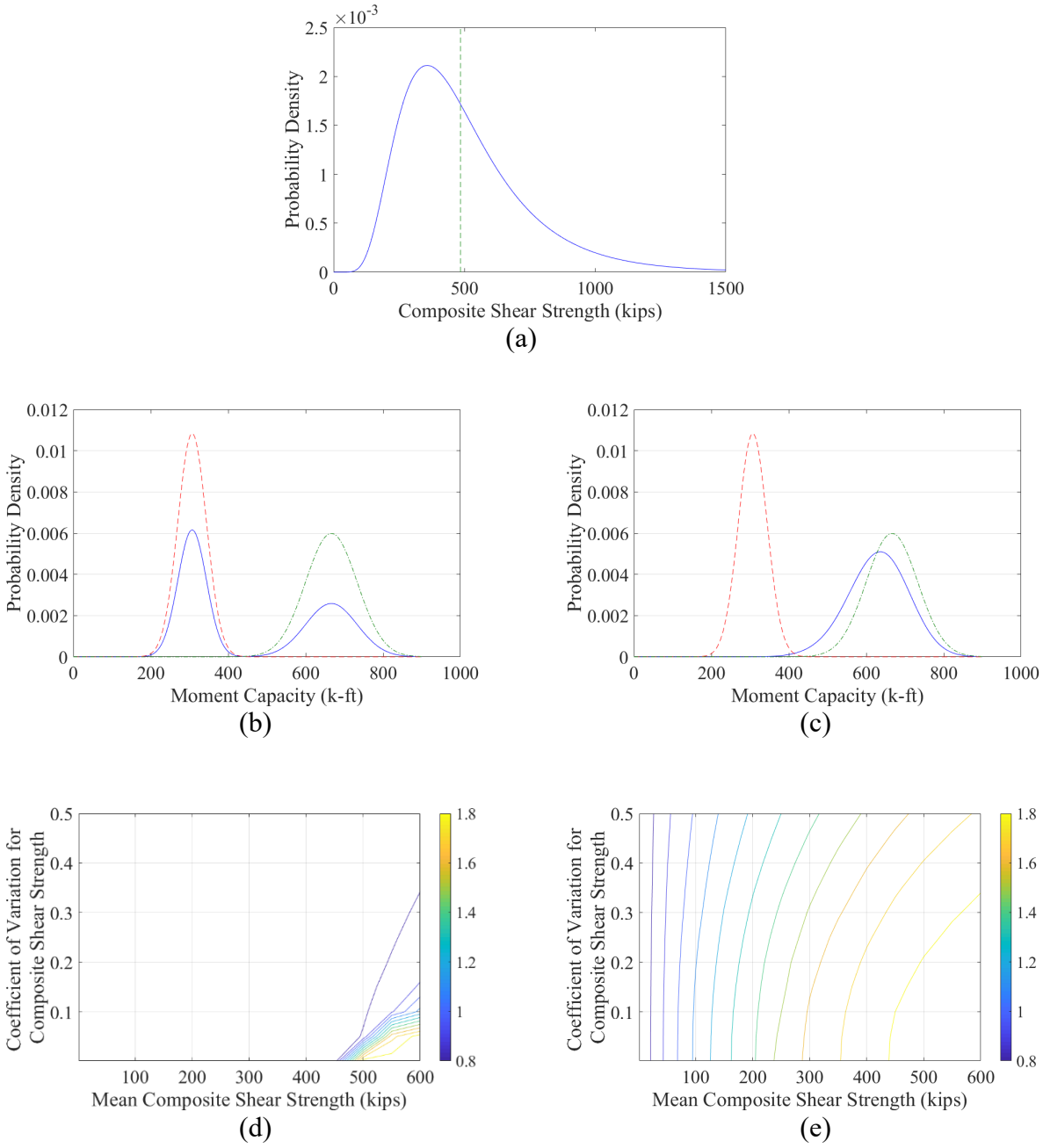

Figure 6. Uncertain Composite Capacity Reliability Analysis: (a) Sample Distribution of Composite Shear Strength (b) Sample Moment Capacity Distribution with Brittle Behavior (c) Sample Moment Capacity Distribution with Ductile Behavior, (d) Rating Factor Contours with Brittle Behavior, and (e) Rating Factor Contours with Ductile Behavior

CONCLUSIONS AND RECOMMENDATIONS

A methodology was outlined and presented with accompanying demonstration results from a case study. The Yutan bridge was load rated as a noncomposite bridge using standard AASHTO line girder analysis. The bridge was assessed to require posting using conventional

methods, so more rigorous analyses were performed. Additionally, preliminary ANNs were used to estimate the expected FEM load rating. The unadjusted ANNs matched closely with the FEM load rating. Reduction factors were presented to account for ANN error. An alternative method was also presented, obtained by performing a reliability calibration to account for increased live load uncertainty with ANN predictions. The reliability calibration method produced a less severe penalty that agreed more closely with refined analysis results.

The unadjusted ANNs showed nearly a 20% benefit compared to AASHTO line girder analysis. Additionally, a load test was performed investigate potential load rating benefits from more favorable moment demands, partial composite behavior, or bearing restraint. It was found that although the bridge was built without shear studs, the deck and girders behaved partially composite in most of the instrumented girders. The partial composite behavior reduced bottom flange stresses, which increased the load rating. A summary of all methods performed is shown in Table 5.

A parametric study was also performed to examine how puddle welds limit behavior could influence the load rating. Reliability analyses were performed for alternate cases with brittle versus ductile limit behavior at the composite shear interface. Brittle behavior was found to result in negligible benefit to the load rating. However, ductile behavior produced rating factors in the range expected with $K_b = 0.5$ or 1. This suggests that the Kb = 0.5 rating factor may be unconservative if puddle weld limit behavior is brittle.

Table 5. Load Rating Comparison

Method	Rating Factor
AASHTO Line Girder	0.85
Single-Best Network Unadjusted	1.02
Committee-Network Unadjusted	0.99
ANSYS	1.04
AASHTO MBE Adjusted $K_b = 0.5$	1.32
AASHTO MBE Adjusted $K_b = 1.0$	1.77

ANNs inherently introduce prediction errors. Only a preliminary study has been performed to account for ANN prediction error uncertainty using structural reliability. However, a project is currently under way that will integrate the ANN uncertainty with the ANN predictions. The ANNs' error can be used to calculate updated coefficient of variation and bias factors. These updated factors can then be used to produce an amplified live load partial safey factor that corresponds to the target reliability index, similar to the original calibration of the AASHTO LRFD code, as described in NCHRP Report 368 (Nowak 1999). It is also

recommended studies be performed to characterize puddle weld composite interface behavior more reliably through small scale testing and, ideally, through field proof load testing.

ACKNOWLEDGEMENTS

This research was conducted with funds from NDOT Project M088. Support for this work, in part, was provided by the National Science Foundation through grant EEC-1659601.

AUTHOR CONTRIBUTIONS

The authors confirm contribution to the paper as follows: methodology: Garcia and Steelman; preliminary analysis and load test: Garcia and Steelman; creating the ANNs used in this study; Sofi and Steelman; puddle weld study; Garfías and Steelman. All authors reviewed the results and approved the final version of the manuscript.

REFERENCES

AASHTO. (2017).*AASHTO LRFD Bridge Design Specifications*,8th Ed., Washington, D.C.

AASHTO.(2010).*The Manual for Bridge Evaluation*, 2nd Ed., 2013 Interim Revisions, Washington, DC.

AASHTO NSBA (2014). *G13.1 Guidelines for Steel Girder Bridge Analysis 2nd Edition*.

Achter, J.L. (2016), "How Effective Are Your Arc Spot Welds?", *Structure*

American Institute of Steel Construction. (2017), *Steel Construction Manual*, 15th ed., American Institute of Steel Construction.

Bridge Engineering Center, BEC. (2010). Diagnostic load testing may reduce embargoes. Iowa State University, Iowa.

Federal Highway Administration, FHWA. (2015). National Bridge Inventory (NBI). U.S.Department of Transportation, Washington, D.C.

Hearn, G. (2014). *NCHRP Synthesis 453: State Bridge Load Posting Processes and Practices*.

Miller, D.K. (2017), *Welded Connections— A Primer for Engineers*, 2nd ed., American Institute of Steel Construction.

Muray, T.M., Allen, D.E. and Ungar, E.E. (1997), *Floor Vibrations Due to Human Activity*, 11th ed., American Institute of Steel Construction.

NCHRP RRD 234 - Lichtenstein Bakht Moses -- Manual for Bridge Rating Through Load Testing – 1998.Nowak, A. (1999). NCHRP Report 368, Calibration of LRFD Bridge Design Code.

Nowak, A. and Collins, K. (2013). *Reliability of Structures*. Boca Raton, Fla.: CRC Press.

Sofi, F. (2017). Structural System-Based Evaluation of Steel Girder Highway Bridges and Artificial Neural Network (ANN) Implementation for Bridge Asset Management. Ph.D. University of Nebraska-Lincoln.

Sofi, F., Lin, X., Steelman, J. and Garcia, F. (2019). *Supporting Bridge Management with Advanced Analysis and Machine Learning*.

Sofi, F. and Steelman, J. (2017). Parametric Influence of Bearing Restraint on Nonlinear Flexural Behavior and Ultimate Capacity of Steel Girder Bridges. *Journal of Bridge Engineering*, 22(7).

Sputo, T., Yantz, D. and Criste, E. (2010), "Attaching Metal Decking", *Steelwise*, Modern Steel Construction

Szerszen, M., Linzell, D., Azam, S., Alhajami, A., Steelman, J. and Wood, R. (2018). Protocol to Evaluate and Load Rate Existing Bridges Using Field Testing.

Vulcraft. (2008), *Steel Floor & Roof Deck*, Vulcraft.

Wipf, T. and Hosteng, T. (2010). *Diagnostic Load Testing May Reduce Embargoes*. Tech Transfer Summary.